Spatial Power Control of Singularly Perturbed Large Nuclear Reactor ⋆

R. K. Munje * **B. M. Patre** **

* *K. K. Wagh Institute of Engineering Education and Research, Amrutdham, Nashik 422003, India. (e-mail: ravimunje@yahoo.co.in).*
** *S. G. G. S. Institute of Engineering and Technology, Vishnupuri, Nanded 431606, India. (e-mail: bmpatre@yahoo.com).*

Abstract: Controlling of large nuclear reactors is a challenging task due to simultaneous presence of both slow and fast varying dynamic modes. This paper presents the design of linear quadratic regulator for spatial power control of a large Advanced Heavy Water Reactor (AHWR). The AHWR system is represented by 90 first order nonlinear differential equations with 5 inputs and 18 outputs. After linearization, the original ill-conditioned system of AHWR is represented into standard singularly perturbed two-time-scale form and decomposed into two comparatively lower order subsystems, namely, 'slow' and 'fast' subsystems of orders 73 and 17 respectively. Two individual optimal controllers are developed for both the subsystems and then a composite controller is obtained for original system. This composite controller is applied to the vectorized nonlinear model of AHWR. From dynamic simulation in representative transients, the suggested controller is found to be superior to other methods.

Keywords: Nuclear reactor, optimal control, order reduction, power control, singular perturbation.

1. INTRODUCTION

The analysis and control of large scale systems have always been a complicated task due coupled variables that evolve in disparate (slow and fast) time-scales. The design of optimal control for such system is impractical. However, this can be achieved by using singular perturbations and time-scale methods (Kokotovic et al. (1976); Saksena et al. (1984)). These methods work by decoupling the fast and slow varying modes. A number of approaches have been developed over the period of time to tackle ill-conditioning generally observed in case of higher order systems (Phillips (1980); Chow et al. (1984); Naidu (1988); Bobasu et al. (2003); Shimjith et al. (2011a)).

In the context of power distribution control in a nuclear reactor, it is worth mentioning that the model of a nuclear reactor belongs to a special class of systems called singularly perturbed systems. The simultaneous presence of both the slow as well as the fast varying dynamical modes, could cause ill-conditioning of the problem. Hence it is necessary to transform the nuclear reactor model into a suitable form whereby stiffness is completely eliminated. Besides, the model order reduction is achieved to a certain extent. Application of singular perturbation techniques to Advanced Heavy Water Reactor (AHWR) and Pressurized Heavy Water Reactor (PHWR) are reported in (Tiwari et al. (1996, 1998); Shimjith et al. (2011a,b); Munje et al. (2013a,b, 2014b)). Some other control techniques suggested for AHWR and PHWR are documented in (Shimjith et al. (2011c); Munje et al. (2014a); Londhe et al. (2014); Abbasi et al. (2014)).

In this paper, the design of a near optimal linear regulator (Chow et al. (1984)) for controlling spatial power in AHWR is proposed, which is then applied to the vectorized nonlinear model of AHWR and simulation results are obtained under different transients. The organization of the paper is as follows. In Section 2 description of AHWR system is given. Control design is proposed in Section 3. In Section 4 application of composite controller to AHWR is presented followed by conclusion in Section 5.

2. DESCRIPTION OF AHWR SYSTEM

2.1 Introduction

In India, Advanced Heavy Water Reactor (AHWR), a 920 MW (thermal), vertical pressure tube type reactor has been designed. It is moderated by heavy water, cooled by boiling light water and fueled with (Th-^{233}U)O_2 and (Th-Pu)O_2 pins (Sinha et al. (2006)). The reactivity control devices in AHWR consist of eight absorber rods (ARs), eight shim rods (SRs) and eight regulating rods (RRs). The physical dimensions of AHWR are large compared to the neutron migration length in the core, making it susceptible to xenon induced spatial oscillations. Spatial oscillations in neutron flux distribution resulting from xenon reactivity feedback are a matter of concern in large nuclear reactors. If the spatial oscillations in power distribution are not controlled, power density and rate of change of power at some locations in the reactor core may exceed limits of fuel failure (Duderstadt and Hamilton (1975)). Spatial control means to suppress xenon oscillations from growing.

⋆ This work was supported by Board of Research in Nuclear Sciences (BRNS), Department of Atomic Energy, Government of India under Grant (Sanction No. 2009/36/102-BRNS).

The objective is to maintain the core power distribution close to a desired shape. For spatial control system design, a very extensive derivation of AHWR mathematical model is given in (Astrom and Bell (2000); Shimjith et al. (2008, 2010)) and the same has been used here for the study carried out in this paper. The AHWR core is considered to be divided in 17 relatively large nodes as shown in Fig. 1. The following nonlinear equations constitute the mathematical model of AHWR:

$$\frac{dW_i}{dt} = (\rho_i - \alpha_{ii} - \beta)\frac{W_i}{\ell} + \sum_{j=1}^{17} \alpha_{ji}\frac{W_j}{\ell} + \lambda C_i \quad (1)$$

$$\frac{dC_i}{dt} = \frac{\beta}{\ell}W_i - \lambda C_i \quad (2)$$

$$\frac{dI_i}{dt} = \gamma_I \Sigma_{fi} W_i - \lambda_I I_i \quad (3)$$

$$\frac{dX_i}{dt} = \gamma_X \Sigma_{fi} W_i + \lambda_I I_i - (\lambda_X + \bar{\sigma}_{Xi} W_i) X_i \quad (4)$$

$$\frac{dH_k}{dt} = \kappa v_k \quad (5)$$

$$e_{vx_i}\frac{dx_i}{dt} = W_i - q_{d_i}(h_w - h_d) - q_{d_i} x_i h_c \quad (6)$$

$$e_{xh}\frac{dh_d}{dt} = q_f(\hat{k}_2 h_f - \hat{k}_1) - q_d(\hat{k}_2 h_d - \hat{k}_1). \quad (7)$$

where $k = 2, 4, 6, 8$ and $i = 1, 2, \ldots, 17$. W, C, I, X and H are nodal powers, effective one group delayed neutron precursor, iodine and xenon concentrations and regulating rod positions respectively. x_i and h_d denote exit quality of i^{th} node and downcomer enthalpy respectively. α_{ji} and α_{ii} denote the coupling coefficients between j^{th} and i^{th} nodes and self coupling coefficients of i^{th} node respectively. $\bar{\sigma}_{Xi} = \sigma_{Xi}/E_{eff}\Sigma_{fi}V_i$ and v_k is control signal applied to the RR drive and κ is a constant having value 0.56. Other notations and symbols have their usual meanings.

Values of e_{vx_i} and e_{xh} along with neutronic parameters, nodal volumes and cross-sections, nodal powers, coolant flow rates under full power operation and coupling coefficients are given in (Shimjith et al. (2011c)). The reactivity term ρ_i in (1) is expressed as $\rho_i = \rho_{i_u} + \rho_{i_X} + \rho_{i_\alpha}$, where ρ_{i_u}, ρ_{i_X} and ρ_{i_α} are the reactivity feedbacks due to the control rods, xenon and coolant void fraction respectively, given by

$$\rho_{i_u} = \begin{cases} (-10.234H_i + 676.203) \times 10^{-6}, & \text{if } i = 2, 4, 6, 8. \\ 0 & \text{elsewhere,} \end{cases}$$

$$\rho_{i_X} = -\frac{\bar{\sigma}_{Xi} X_i}{\Sigma_{ai}},$$

$$\begin{aligned}\rho_{i_\alpha} = & -5 \times 10^{-3}(9.2832x_i^5 - 27.7192x_i^4 + 31.7643x_i^3 \\ & -17.7389x_i^2 + 5.2308x_i + 0.0792).\end{aligned}$$

Equations (1)-(7) are linearized around steady state operating conditions $(H_{k_0}, X_{i_0}, I_{i_0}, h_{d_0}, C_{i_0}, x_{i_0}, W_{i_0})$ and represented in standard state space form. For this, define the state vector as

$$\mathbf{z} = \left[\, z_H^T \; z_X^T \; z_I^T \; \delta h_d \; z_C^T \; z_x^T \; z_W^T \,\right]^T \quad (8)$$

where $z_H = [\, \delta H_2 \; \delta H_4 \; \delta H_6 \; \delta H_8 \,]^T$ and the rest $\mathbf{z}_\xi = [\, (\delta\xi_1/\xi_{1_0}) \cdots (\delta\xi_{17}/\xi_{17_0}) \,]^T$, $\xi = X, I, C, x, W$, in which δ denotes the deviation from respective steady state value of the variable. Likewise, define the input vector as $\mathbf{u} = [\, \delta v_2 \; \delta v_4 \; \delta v_6 \; \delta v_8 \,]^T$ and output vector as $\mathbf{y} = [\, y_g \; y_1 \; \cdots \; y_{17} \,]^T$ where $y_g = \sum_{i=1}^{17} \frac{\delta W_i}{\sum_{j=1}^{17} W_{j_0}}$ and $y_i = \frac{\delta W_i}{W_{i_0}}$ correspond to normalized total reactor power and nodal powers respectively. Then, the system given by (1)-(7) can be expressed in standard linear state space form as

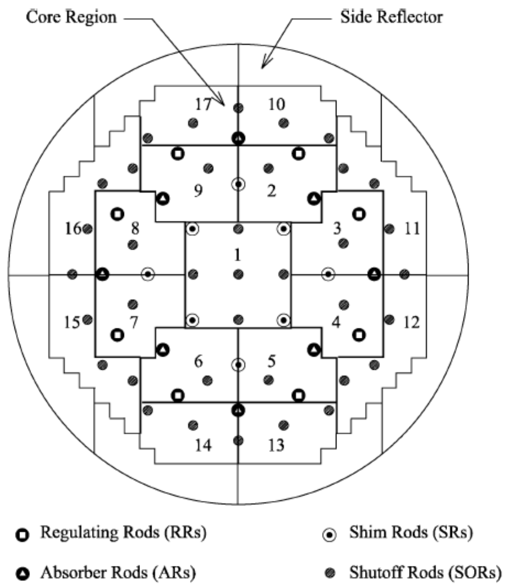

Fig. 1. 17 nodes AHWR scheme.

$$\dot{\mathbf{z}} = \mathbf{A}\mathbf{z} + \mathbf{B}\mathbf{u} + \mathbf{B}_{fw}\delta q_{fw} \quad (9)$$

$$\mathbf{y} = \mathbf{M}\mathbf{z} \quad (10)$$

where δq_{fw} is deviation in feed water flow rate. Matrices $\mathbf{A}$, $\mathbf{B}$, $\mathbf{B}_{fw}$ and $\mathbf{M}$ are given in (Shimjith et al. (2011c)). Eigenvalues of $\mathbf{A}$ fall in two distinct clusters. First cluster has 73 eigenvalues ranging from -1.8395×10^{-1} to 3.9654×10^{-6} and the second one is of 17 eigenvalues ranging from -2.7626×10^2 to -7.2516. Six eigenvalues of $\mathbf{A}$ have their real parts positive while four eigenvalues are at the origin (grouped in first cluster), which indicates instability. Hence, it is necessary to design an effective controller to maintain the total power of the reactor while the xenon induced oscillations are being controlled.

2.2 *Control Problem of AHWR*

Spatial control of AHWR has been attempted by Shimjith et al. (2011c); Munje et al. (2014a) using output feedback based technique. However, static output feedback does not guarantee the stability of closed loop system (Syrmos et al. (1997)). As an extension to this a state feedback based three-time-scale approach has been applied to AHWR in (Shimjith et al. (2011a)). In this quasi-steady-state method is used to decouple the AHWR system in 'slow', 'fast 1' and 'fast 2' subsystems. The practical implementation of such a state feedback based controller demands a state observer of large order. Hence, Fast Output Sampling (FOS) based controller is investigated in (Shimjith et al.

(2011b)). This method is based on Multirate Output Feedback (MROF), by which the states of the system can be computed exactly. In FOS, control signal is generated as a linear combination of a number of output samples collected in one sampling interval. In this, input sampling time is larger compared to output sampling time. For example in (Shimjith et al. (2011b)), sampling time for spatial control component of input is taken as 60 s. A similar kind of approach for two-time-scale system is suggested in (Munje et al. (2013a)) for the AHWR, where sampling time is taken as 54 s. However, for practical reactor control to work with larger sampling time is not desirable, because in small time, reactor can undergo a considerable change. Hence, Periodic Output Feedback (POF) technique, duel of FOS, is suggested in (Munje et al. (2014b)). These MROF based methods (i.e. FOS and POF) have their own advantages, but they lack robustness. These methods may not work satisfactorily in the presence of disturbance, parameter variations and perturbations in the operating conditions. Therefore, robust sliding mode control (SMC) technique is explored for AHWR in (Munje et al. (2013b)) and it is shown that, better results are obtained. However, it requires all the states for feedback. Recently, single-input fuzzy logic controller is also suggested for control of AHWR (Londhe et al. (2014)), in which feedback of 24 states is used to drive the AHWR system.

In this paper, model order reduction has been carried out via two-time-scale decomposition to obtain reduced order subsystems of AHWR. In contrast to the earlier work of (Shimjith et al. (2011a)), where three-time-scale decomposition method was used to obtain three subsystems, this method provides higher degree of accuracy. Moreover, the comparison of results, helps to understand the effect of different model order reduction methods.

3. CONTROL DESIGN

Singularly perturbed systems can be modeled by set of nonlinear differential equations (Kokotovic et al. (1976); Saksena et al. (1984)) given by

$$\dot{\mathbf{z}}_1 = f(\mathbf{z}_1, \mathbf{z}_2, \mathbf{u}, t); \quad \mathbf{z}_1(t_0) = \mathbf{z}_{1_0}, \tag{11}$$

$$\varepsilon\dot{\mathbf{z}}_2 = g(\mathbf{z}_1, \mathbf{z}_2, \mathbf{u}, t); \quad \mathbf{z}_2(t_0) = \mathbf{z}_{2_0}, \tag{12}$$

$$\mathbf{y} = h(\mathbf{z}_1, \mathbf{z}_2, \mathbf{u}, t) \tag{13}$$

where the n_1 dimensional state vector $\mathbf{z}_1$ is predominantly slow and the n_2 dimensional state vector $\mathbf{z}_2$ contains fast transients superimposed on a slowly varying "quasi-steady-state", i.e. $\|\dot{\mathbf{z}}_1 \gg \dot{\mathbf{z}_2}\|$, such that $n_1 + n_2 = n$, $\mathbf{u} \in \Re^m$ is the input, $\mathbf{y} \in \Re^p$ is the output, parameter $\varepsilon > 0$ is a scalar representing the speed ratio of the slow versus fast phenomenon. The model represented by (11)-(13) is a standard singularly perturbation model extensively studied in control literature. As the parameter ε tends to zero, the solution behaves non-uniformly, producing so called singularly perturbed stiff problem. The scalar ε represents all the small parameters to be neglected. The parameter ε can be picked up on the basis of knowledge of the process/system and components. A linear time-invariant controllable and observable version, obtained by linearizing (11)-(13) has the form

$$\dot{\mathbf{z}}_1 = \mathbf{A}_{11}\mathbf{z}_1 + \mathbf{A}_{12}\mathbf{z}_2 + \mathbf{B}_1\mathbf{u}, \tag{14}$$

$$\varepsilon\dot{\mathbf{z}}_2 = \mathbf{A}_{21}\mathbf{z}_1 + \mathbf{A}_{22}\mathbf{z}_2 + \mathbf{B}_2\mathbf{u}, \tag{15}$$

$$\mathbf{y} = \mathbf{M}_1\mathbf{z}_1 + \mathbf{M}_2\mathbf{z}_2 \tag{16}$$

where the matrices $\mathbf{A}_{ij}$, $\mathbf{B}_i$ and $\mathbf{M}_i$ are of appropriate dimensionality.

3.1 Two-Time-Scale Decomposition

The separation of states into slow and fast is nontrivial modeling task demanding insight and ingenuity on the part of the analyst. The main purpose of singularly perturbation approach to analysis and design is the alleviation of high dimensionality and ill-conditioning resulting from the interactions of slow and fast dynamic modes. For grouping of state variables of the physical system into slow and fast groups, a method based on scaling of state has been proposed in (Chow et al. (1984)). Now setting $\varepsilon = 0$, the system (14)-(16) can be decomposed into two subsystems as follows.

Slow subsystem: The slow subsystem is represented by

$$\dot{\mathbf{z}}_s = \mathbf{A}_s\mathbf{z}_s + \mathbf{B}_s\mathbf{u}_s \tag{17}$$

$$\mathbf{y}_s = \mathbf{M}_s\mathbf{z}_s + \mathbf{N}_s\mathbf{u}_s \tag{18}$$

where

$$\mathbf{A}_s = \mathbf{A}_{11} - \mathbf{A}_{12}\mathbf{A}_{22}^{-1}\mathbf{A}_{21}, \mathbf{B}_s = \mathbf{B}_1 - \mathbf{A}_{12}\mathbf{A}_{22}^{-1}\mathbf{B}_2,$$
$$\mathbf{M}_s = \mathbf{M}_1 - \mathbf{M}_2\mathbf{A}_{22}^{-1}\mathbf{A}_{21}, \mathbf{N}_s = -\mathbf{M}_2\mathbf{A}_{22}^{-1}\mathbf{B}_2.$$

Fast subsystem: The fast subsystem model is given by

$$\frac{d\mathbf{z}_f}{d\tau_\varepsilon} = \mathbf{A}_f\mathbf{z}_f + \mathbf{B}_f\mathbf{u}_f \tag{19}$$

$$\mathbf{y}_f = \mathbf{M}_f\mathbf{z}_f \tag{20}$$

where $\mathbf{A}_f = \mathbf{A}_{22}$, $\mathbf{B}_f = \mathbf{B}_2$ and $\mathbf{M}_f = \mathbf{M}_2$. Note that the slow subsystem is of order n_1 and the fast subsystem is of order n_2.

3.2 Linear State Feedback Control

For convenience system (14)-(16) is again represented in the following form

$$\dot{\mathbf{z}} = \mathbf{A}\mathbf{z} + \mathbf{B}\mathbf{u} \tag{21}$$

$$\mathbf{y} = \mathbf{M}\mathbf{z} \tag{22}$$

where $\mathbf{z} = \left[\, \mathbf{z}_1^T \ \mathbf{z}_2^T \,\right]^T$ is the $n_1 + n_2 = n$ dimensional state vector and recall that

$$\mathbf{A} = \begin{bmatrix} \mathbf{A}_{11} & \mathbf{A}_{12} \\ \frac{\mathbf{A}_{21}}{\varepsilon} & \frac{\mathbf{A}_{22}}{\varepsilon} \end{bmatrix}, \mathbf{B} = \begin{bmatrix} \mathbf{B}_1 \\ \frac{\mathbf{B}_2}{\varepsilon} \end{bmatrix}, \mathbf{M} = \begin{bmatrix} \mathbf{M}_1 \\ \mathbf{M}_2 \end{bmatrix}^T. \tag{23}$$

In particular, it is considered to minimize the quadratic performance index

$$J = \int_0^\infty \left[\, \mathbf{z}^T\mathbf{Q}\mathbf{z} + \mathbf{u}^T\mathbf{R}\mathbf{u} \,\right] dt \tag{24}$$

where $\mathbf{Q} \geq 0$ and $\mathbf{R} > 0$ are respectively $(n \times n)$ and $(m \times m)$ matrices. The solution to the problem (24) is the optimal linear feedback law

$$\mathbf{u} = -\mathbf{R}^{-1}\mathbf{B}^T\mathbf{S}\left[\,\mathbf{z}_1^T \;\; \mathbf{z}_2^T\,\right]^T$$
$$= \mathbf{K}_{opt}\left[\,\mathbf{z}_1^T \;\; \mathbf{z}_2^T\,\right]^T = \mathbf{K}_{opt}\mathbf{z} \quad (25)$$

where $(n \times n)$ matrix $\mathbf{S}$ in (25) can be obtained by solving the Riccati equation

$$\mathbf{S}\mathbf{A} + \mathbf{A}^T\mathbf{S} - \mathbf{S}\mathbf{B}\mathbf{R}^{-1}\mathbf{B}^T\mathbf{S} + \mathbf{Q} = 0. \quad (26)$$

Several methods are available for solving the Algebraic Matrix Riccati equation (26). However, the enormous size of the problem and the stiffness due to the presence of both the slow and fast dynamic phenomenon cripple even the most effective approach. Hence, by application of singular perturbation approach, the original higher order ill-conditioned system is decomposed in two subsystems and the linear regulator design is carried out for two separate subsystems individually. Finally separately designed regulators are combined to obtain control law given by (25). For design purpose, the matrices $\mathbf{Q}$ and $\mathbf{S}$ are assumed to be partitioned as

$$\mathbf{Q} = \begin{bmatrix} \mathbf{Q}_{11} & \mathbf{Q}_{12} \\ \mathbf{Q}_{12}^T & \mathbf{Q}_{22} \end{bmatrix} \text{ and } \mathbf{S} = \begin{bmatrix} \mathbf{S}_{11} & \varepsilon\mathbf{S}_{12} \\ \varepsilon\mathbf{S}_{12}^T & \varepsilon\mathbf{S}_{22} \end{bmatrix}. \quad (27)$$

Substituting the values of $\mathbf{Q}$ and $\mathbf{S}$ from (27) along with $\mathbf{A}$ and $\mathbf{B}$, from (23), and then simplifying with the assumption $\varepsilon = 0$, the original problem decomposes into two linear regulator problems as described in the following.

Fast subsystem regulator problem: For fast subsystem (19), control is given by

$$\mathbf{u}_f = -\mathbf{R}^{-1}\mathbf{B}_f^T\mathbf{S}_{22}\mathbf{z}_f = \mathbf{K}_2\mathbf{z}_f \quad (28)$$

where

$$\mathbf{S}_{22}\mathbf{A}_f + \mathbf{A}_f^T\mathbf{S}_{22} - \mathbf{S}_{22}\mathbf{B}_f\mathbf{R}^{-1}\mathbf{B}_f^T\mathbf{S}_{22} + \mathbf{Q}_f = 0 \quad (29)$$

where $\mathbf{Q}_f = \mathbf{Q}_{22} \geq 0$ and $\mathbf{R} > 0$. A unique solution of $\mathbf{S}_{22}$ exists if the fast subsystem pair $(\mathbf{A}_f, \mathbf{B}_f)$ is controllable.

Slow subsystem regulator problem: The optimal control for slow subsystem (17) is given by

$$\mathbf{u}_s = -\mathbf{R}_0^{-1}\left(\mathbf{H}_0 + \mathbf{B}_0^T\mathbf{S}_0\right)\mathbf{z}_s = \mathbf{K}_0\mathbf{z}_s \quad (30)$$

where $\mathbf{S}_0$ is obtained by solving

$$\mathbf{S}_0\mathbf{A}_0 + \mathbf{A}_0^T\mathbf{S}_0 - \mathbf{S}_0\mathbf{B}_0\mathbf{R}_0^{-1}\mathbf{B}_0^T\mathbf{S}_0 + \mathbf{Q}_0 = 0 \quad (31)$$

in which

$$\begin{aligned}
\mathbf{A}_0 &= \mathbf{A}_s - \mathbf{B}_s\mathbf{R}_0^{-1}\mathbf{H}_0,\\
\mathbf{B}_0 &= \mathbf{B}_s,\\
\mathbf{Q}_0 &= \bar{\mathbf{Q}}_0 - \mathbf{H}_0^T\mathbf{R}_0^{-1}\mathbf{H}_0,\\
\mathbf{R}_0 &= \mathbf{R} + \left(\mathbf{A}_{22}^{-1}\mathbf{B}_f\right)^T\mathbf{Q}_{22}\mathbf{A}_{22}^{-1}\mathbf{B}_f,\\
\mathbf{H}_0 &= -\left(\mathbf{A}_{22}^{-1}\mathbf{B}_f\right)^T\left[\mathbf{Q}_{12}^T - \mathbf{Q}_{22}\mathbf{A}_{22}^{-1}\mathbf{A}_{21}\right],\\
\bar{\mathbf{Q}}_0 &= \mathbf{Q}_{11} - \mathbf{Q}_{12}\mathbf{A}_{22}^{-1}\mathbf{A}_{21} - \left(\mathbf{A}_{22}^{-1}\mathbf{A}_{21}\right)^T\\
&\quad \left[\mathbf{Q}_{12}^T - \mathbf{Q}_{22}\mathbf{A}_{22}^{-1}\mathbf{A}_{21}\right].
\end{aligned}$$

Composite Controller Design: Separately designed optimal controllers (28) and (30) should ensure the stability of subsystems i.e.

$$\Re e\left[\,\varphi(\mathbf{A}_f + \mathbf{B}_f\mathbf{K}_2) < 0\,\right] \quad (32)$$
$$\text{and } \Re e\left[\,\varphi(\mathbf{A}_s + \mathbf{B}_s\mathbf{K}_0) < 0\,\right] \quad (33)$$

where $\varphi(.)$ is eigenvalue. As a result, an asymptotically stable closed loop behavior can be obtained if the following composite control is applied to the system (14)-(15)

$$\mathbf{u} = \mathbf{K}_0\mathbf{z}_s + \mathbf{K}_2\mathbf{z}_f. \quad (34)$$

In terms of states $\mathbf{z}_1$ and $\mathbf{z}_2$, one can write

$$\mathbf{u} = \left[\,(\mathbf{E}_m + \mathbf{K}_2\mathbf{A}_{22}^{-1}\mathbf{B}_2)\mathbf{K}_0 + \mathbf{K}_2\mathbf{A}_{22}^{-1}\mathbf{A}_{21}\,\right]\mathbf{z}_1 + \mathbf{K}_2\mathbf{z}_2$$
$$= \left[\,\mathbf{K}_1 \;\; \mathbf{K}_2\,\right]\left[\,\mathbf{z}_1^T \;\; \mathbf{z}_2^T\,\right]^T \quad (35)$$

where $\mathbf{K}_1 = (\mathbf{E}_m + \mathbf{K}_2\mathbf{A}_{22}^{-1}\mathbf{B}_2)\mathbf{K}_0 + \mathbf{K}_2\mathbf{A}_{22}^{-1}\mathbf{A}_{21}$, in which $\mathbf{E}_m$ is $(m \times m)$ identity matrix. Further (35) can be written as

$$\mathbf{u} = \mathbf{K}_{opt}\mathbf{z} \quad (36)$$

where $\mathbf{K}_{opt} = [\,\mathbf{K}_1 \;\; \mathbf{K}_2\,]$. This composite control can serve as a near optimum control for the actual higher order system.

Remark 1: If the system is having stable fast modes, then $\mathbf{K}_2$ can be taken as null matrix of $(m \times n_2)$ dimension. This yields reduced two-time-scale approximation to $\mathbf{K}_{opt}$ as $\bar{\mathbf{K}}_{opt} = [\,\mathbf{K}_0 \;\; \mathbf{0}\,]$.

4. APPLICATION TO AHWR

The linear model of the AHWR given by (9)-(10) is found to controllable and observable (Shimjith et al. (2011c)). The control input $\mathbf{u}$, to RR drives consist of two terms, written as

$$\mathbf{u} = \mathbf{u}_{gp} + \mathbf{u}_{sp} \quad (37)$$

where $\mathbf{u}_{gp}$ is global power component, designed in (Munje et al. (2013b)), and $\mathbf{u}_{sp}$ is spatial power feedback component. After application of global and spatial power feedbacks system (9) becomes

$$\dot{\mathbf{z}} = \hat{\mathbf{A}}\mathbf{z} + \mathbf{B}\mathbf{u}_{sp} + \mathbf{B}_{fw}\delta q_{fw} \quad (38)$$

where $\hat{\mathbf{A}}$, system matrix with global power feedback (Shimjith et al. (2011c)), has eigenvalues falling in two distinct clusters. First cluster of 73 eigenvalues ranging from -1.8402×10^{-1} to -2.6799×10^{-5} with three eigenvalues at origin and second cluster of 17 eigenvalues range from -7.2484 to -2.7626×10^{2}. Hence, it is possible to transform model (38) into singularly perturbed form (14)-(15).

4.1 Singularly Perturbed Form of AHWR Model

In case of AHWR, after linearization of set of equations given by (1)-(7), it is indeed observed that coefficients in the 17 equations for nodal powers, contain ℓ in their denominator. It is neutron life time and its value is 3.6694×10^{-4} s. This parameter can be picked up as ε. Therefore, the state variables of system defined by (8) are grouped into slow and fast ones as

$$\mathbf{z}_1 = \left[\,\mathbf{z}_H^T \;\; \mathbf{z}_X^T \;\; \mathbf{z}_I^T \;\; \delta h_d \;\; \mathbf{z}_C^T \;\; \mathbf{z}_x^T\,\right]^T, \quad (39)$$
$$\mathbf{z}_2 = \mathbf{z}_W. \quad (40)$$

Now, the AHWR model is transformed into standard singularly perturbed two-time-scale form, given by (14)-(15), where $n_1 = 73$ and $n_2 = 17$. Submatrices $\mathbf{A}_{11}$, $\mathbf{A}_{12}$, $\frac{\mathbf{A}_{21}}{\varepsilon}$, $\frac{\mathbf{A}_{22}}{\varepsilon}$, $\mathbf{B}_1$ and $\frac{\mathbf{B}_2}{\varepsilon}$ are respectively of dimensions (73×73), (73×17), (17×73), (17×17), (73×4) and (17×4).

4.2 Composite Controller Design

Now model (38) is decomposed into slow and fast subsystems, using equations (17)-(20). The eigenvalues of matrices $\mathbf{A}_s$ and $\mathbf{A}_f$ are given in Tables (1) and (2) respectively. It is seen that the eigenvalues of the fast subsystem matrix $\mathbf{A}_f$ are in excellent agreement with the last 17 eigenvalues of matrix $\hat{\mathbf{A}}$. Similarly, the slow subsystem eigenvalues compare well with remaining 73 eigenvalues of matrix $\hat{\mathbf{A}}$. Hence, it can be concluded that the singularly perturbed form of model (38) is valid in case of AHWR. Slow subsystem contains the eigenvalues which are unstable along with those near the origin whereas fast subsystem contains stable eigenvalues. It may further be noticed that in comparison with (14)-(16), the submatrix $\mathbf{B}_2$ of the input matrix is null matrix, thereby leading to $\mathbf{B}_f = 0$. In other words, the fast subsystem is uncontrollable. However, it can be verified that the slow subsystem is controllable and hence only $\mathbf{K}_0$ needs to be designed for system (38) as given below

$$\mathbf{u}_{sp} = \mathbf{K}_0 \mathbf{z}_1. \tag{41}$$

The regulator design is carried out using equations described in Sections 3.2 with $\mathbf{R}$ as a (4×4) identity matrix and the matrix $\mathbf{Q}$ as given in (Shimjith et al. (2011a)). The matrix $\mathbf{S}_0$ is evaluated by solving (31) and the optimal control gain $\mathbf{K}_0$ for the slow subsystem is determined from (30). Finally the composite gain matrix $\mathbf{K}_{opt}$ is determined from (35) and is given by

$$\mathbf{K}_{opt} = -\left[\, \mathbf{K}_H \ \mathbf{K}_X \ \mathbf{K}_I \ \mathbf{K}_h \ \mathbf{K}_C \ \mathbf{K}_x \ \mathbf{0} \,\right] \tag{42}$$

where $\mathbf{0}$ denotes a null matrix of (4×17) order and $\mathbf{K}_H$, $\mathbf{K}_X$, $\mathbf{K}_I$, $\mathbf{K}_h$, $\mathbf{K}_C$ and $\mathbf{K}_x$ are feedback gains corresponding to RR positions, xenon, iodine, enthalpy, delayed neutron precursor and exit quality respectively. With global power feedback and (42), the overall control input (37) becomes

$$\mathbf{u} = -\mathbf{K}_H \mathbf{z}_H - \mathbf{K}_X \mathbf{z}_X - \mathbf{K}_I \mathbf{z}_I - \mathbf{K}_h \mathbf{z}_h \tag{43}$$

$$-\mathbf{K}_C \mathbf{z}_C - \mathbf{K}_x \mathbf{z}_x + \mathbf{u}_{gp}. \tag{44}$$

Table (3) lists the closed loop eigenvalues of (38), which shows that all the eigenvalues are in left half of s-plane.

4.3 Transient Simulations

Response of the controller was analyzed by simulating the vectorized nonlinear model (Munje et al. (2014a)) of AHWR given by (1)-(7) in MATLAB/Simulink for the transients involving a disturbance in the spatial power distribution. The reactor was assumed to be initially operating at full power equilibrium condition. Shortly, RR2, originally under auto control, was driven out manually by 1% giving appropriate control signal after 2 s and thereafter left on auto control as shown in Fig. 2. Other

Table 1. Eigenvalues of slow subsystem ($\mathbf{A}_s$).

Sr. No.	Eigenvalues	Sr. No.	Eigenvalues
1	2.4139×10^{-17}	42	-5.7898×10^{-2}
2	6.1105×10^{-17}	43	-5.9709×10^{-2}
3	-2.2396×10^{-17}	44	-5.9727×10^{-2}
4	-2.8757×10^{-5}	45	-6.0346×10^{-2}
5	-3.7781×10^{-5}	46	-6.0644×10^{-2}
6	-3.7993×10^{-5}	47	-6.1849×10^{-2}
7	-4.0124×10^{-5}	48	-6.1946×10^{-2}
8	-4.1520×10^{-5}	49	-6.2200×10^{-2}
9	-4.1968×10^{-5}	50	-6.2385×10^{-2}
10	-4.4204×10^{-5}	51	-6.2458×10^{-2}
11	-4.7338×10^{-5}	52	-6.2608×10^{-2}
12	-4.8866×10^{-5}	53	-6.2865×10^{-2}
13-14	$(-7.7407\pm$ i $2.9929)\times10^{-5}$	54	-6.2894×10^{-2}
15-16	$(-7.3360\pm$ i $3.9319)\times10^{-5}$	55	-9.7168×10^{-2}
17-18	$(-6.4855\pm$ i $5.3109)\times10^{-5}$	56	-1.0708×10^{-1}
19-20	$(-3.5444\pm$ i $7.7360)\times10^{-5}$	57	-1.3169×10^{-1}
21-22	$(-3.7785\pm$ i $7.6475)\times10^{-5}$	58	-1.4712×10^{-1}
23-24	$(-6.5949\pm$ i $5.4819)\times10^{-5}$	59	-1.4713×10^{-1}
25-26	$(\ 8.0471\pm$ i $3.9863)\times10^{-5}$	60	-1.4808×10^{-1}
27-28	$(\ 8.8268\pm$ i $2.1800)\times10^{-5}$	61	-1.5063×10^{-1}
29	-1.4107×10^{-4}	62	-1.5580×10^{-1}
30	-1.4441×10^{-4}	63	-1.5585×10^{-1}
31	-1.5717×10^{-4}	64	-1.5662×10^{-1}
32	-1.6524×10^{-4}	65	-1.6019×10^{-1}
33	-1.6573×10^{-4}	66	-1.6316×10^{-1}
34	-1.7308×10^{-4}	67	-1.6324×10^{-1}
35	-1.8807×10^{-4}	68	-1.6404×10^{-1}
36	-1.8870×10^{-4}	69	-1.7531×10^{-1}
37	-2.4408×10^{-4}	70	-1.8031×10^{-1}
38	-1.5738×10^{-2}	71	-1.8049×10^{-1}
39	-5.0954×10^{-2}	72	-1.8122×10^{-1}
40	-5.1179×10^{-2}	73	-2.7823×10^{-1}
41	-5.7743×10^{-2}		

Table 2. Eigenvalues of fast subsystem ($\mathbf{A}_f$).

Sr. No.	Eigenvalues	Sr. No.	Eigenvalues	Sr. No.	Eigenvalues
1	-7.2028	7	-9.4608×10^{1}	13	-2.1110×10^{2}
2	-3.2833×10^{1}	8	-1.0868×10^{2}	14	-2.1904×10^{2}
3	-3.3361×10^{1}	9	-1.1704×10^{2}	15	-2.3591×10^{2}
4	-6.6593×10^{1}	10	-1.6967×10^{2}	16	-2.7163×10^{2}
5	-6.8317×10^{1}	11	-1.7568×10^{2}	17	-2.7626×10^{2}
6	-9.3649×10^{1}	12	-1.9497×10^{2}		

RRs moved in under the effect of the controller in order to maintain the total reactor power. After the period during which the manual signal was enforced on RR2, all RRs were being driven by the controller to their original positions within 135 s. Variations in spatial power measured in terms of first and second azimuthal tilts (Shimjith et al. (2011c)) along with variations in quadrant powers and global power are shown in Figs. 3, 4 and 5 respectively.

In order to assess the response of the system to disturbance in feed flow, the model was simulated when 5% positive step change was introduced in the feed flow as shown in Fig. 6(a). As a result of this, the incoming coolant enthalpy reduced by about 0.64% (Fig. 6(b)). The total power was found to be stabilizing at its rated value due to the action of controller (Fig. 6(c)). However, RRs are driven in by 0.9% (Fig. 6(d)). For the temporary disturbance introduced in feed flow the total power is found to be stabilizing back at their original value and RRs also came back to their equilibrium positions as illustrated in Fig 7.

Table 3. Closed loop eigenvalues of the AHWR model.

Sr. No.	Eigenvalues	Sr. No.	Eigenvalues
1	-2.8369×10^{-5}	50	-6.2865×10^{-2}
2-3	$(-3.6054\pm$ i $7.7099)\times10^{-5}$	51	-6.2893×10^{-2}
4-5	$(-3.9491\pm$ i $7.5495)\times10^{-5}$	52	-5.0944×10^{-2}
6	-3.7779×10^{-5}	53	-5.1151×10^{-2}
7	-3.7985×10^{-5}	54	-1.5738×10^{-2}
8	-4.1515×10^{-5}	55	-9.6913×10^{-2}
9	-4.1942×10^{-5}	56	-1.3225×10^{-1}
10	-4.0111×10^{-5}	57	-1.4712×10^{-1}
11	-4.4291×10^{-5}	58	-1.4713×10^{-1}
12	-4.7331×10^{-5}	59	-1.4809×10^{-1}
13	-4.9080×10^{-5}	60	-1.5068×10^{-1}
14-15	$(-6.5115\pm$ i $5.2628)\times10^{-5}$	61	-1.5580×10^{-1}
16-17	$(-6.5926\pm$ i $5.4855)\times10^{-5}$	62	-1.5585×10^{-1}
18-19	$(-7.3405\pm$ i $3.9069)\times10^{-5}$	63	-1.5662×10^{-1}
20-21	$(-7.7414\pm$ i $2.9910)\times10^{-5}$	64	-1.6022×10^{-1}
22-23	$(-8.3203\pm$ i $3.3684)\times10^{-5}$	65	-1.6316×10^{-1}
24	-8.4318×10^{-5}	66	-1.6324×10^{-1}
25	-9.6873×10^{-5}	67	-1.6405×10^{-1}
26	-1.4048×10^{-4}	68	-1.7542×10^{-1}
27	-1.4459×10^{-4}	69	-1.8037×10^{-1}
28	-1.5742×10^{-4}	70	-1.8049×10^{-1}
29	-1.6516×10^{-4}	71	-1.8122×10^{-1}
30	-1.6590×10^{-4}	72	-2.8889×10^{-1}
31	-1.7323×10^{-4}	73	-1.0800×10^{-1}
32	-1.8816×10^{-4}	74	-6.9171×10^{0}
33	-1.8871×10^{-4}	75	-3.2844×10^{1}
34	-2.4746×10^{-4}	76	-3.3372×10^{1}
35	-7.9732×10^{-3}	77	-6.6599×10^{1}
36	-8.0749×10^{-3}	78	-6.8323×10^{1}
37	-8.1030×10^{-3}	79	-9.4612×10^{1}
38	-5.7736×10^{-2}	80	-9.3653×10^{1}
39	-5.7892×10^{-2}	81	-1.0868×10^{2}
40	-5.9706×10^{-2}	82	-1.1705×10^{2}
41	-5.9723×10^{-2}	83	-1.6967×10^{2}
42	-6.0344×10^{-2}	84	-1.7568×10^{2}
43	-6.0642×10^{-2}	85	-1.9497×10^{2}
44	-6.1848×10^{-2}	86	-2.1110×10^{2}
45	-6.1945×10^{-2}	87	-2.1904×10^{2}
46	-6.2200×10^{-2}	88	-2.3591×10^{2}
48	-6.2458×10^{-2}	89	-2.7163×10^{2}
49	-6.2608×10^{-2}	90	-2.7626×10^{2}
47	-6.2384×10^{-2}		

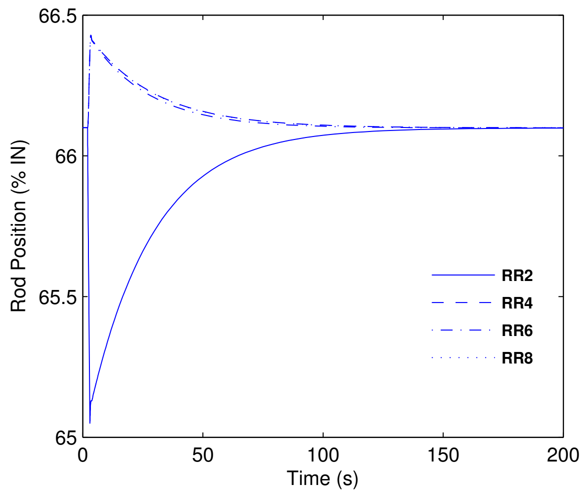

Fig. 2. Variation in RR positions during the transient.

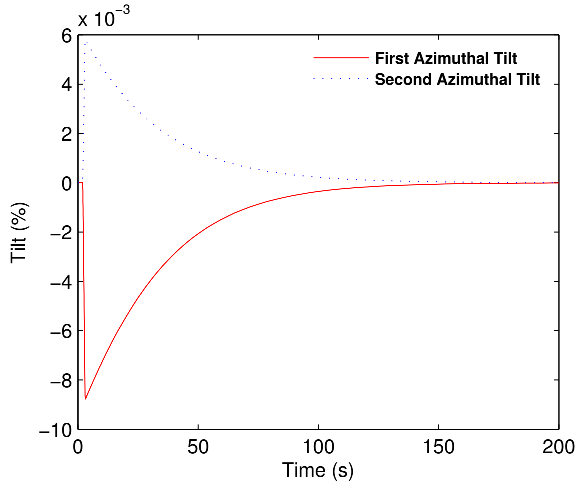

Fig. 3. Suppression of tilts initiated by change in position of RR2.

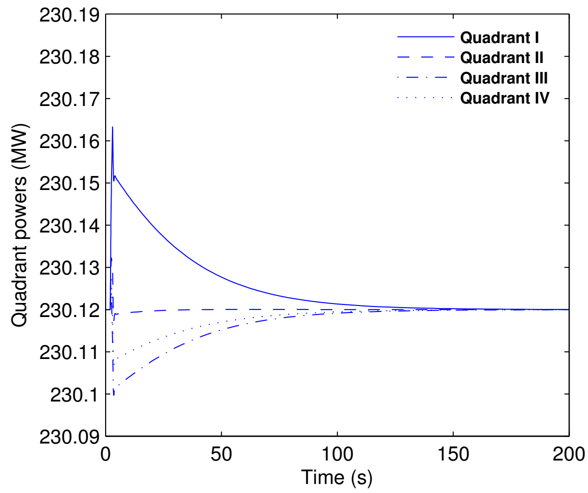

Fig. 4. Quadrant power variations during the transient.

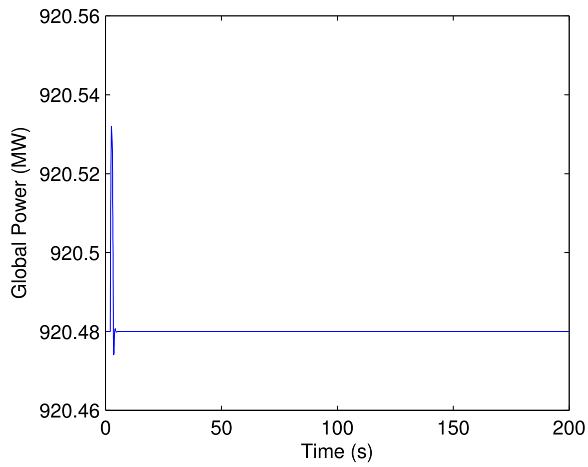

Fig. 5. Variations in global power during the transient.

In another transient, initially, the reactor is under steady state and is assumed to be operating at 920.48 MW with nodal power distribution as given in Shimjith et al. (2011c). Now, the demand is reduced uniformly at the rate

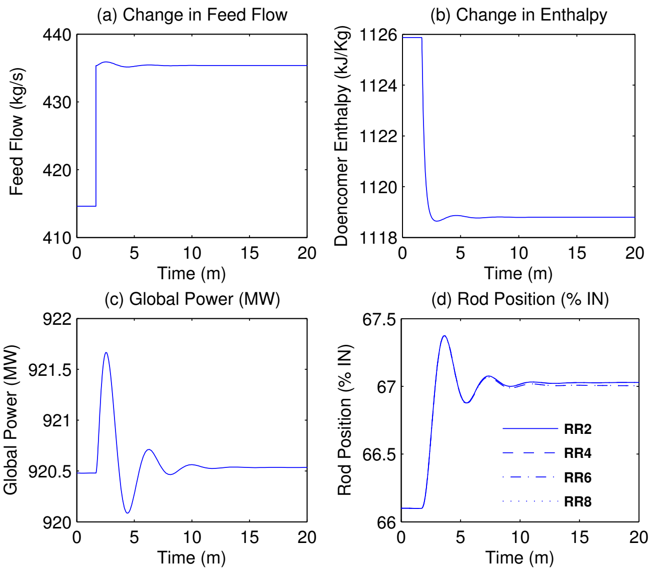

Fig. 6. Effect of 5% positive step change in the feed flow.

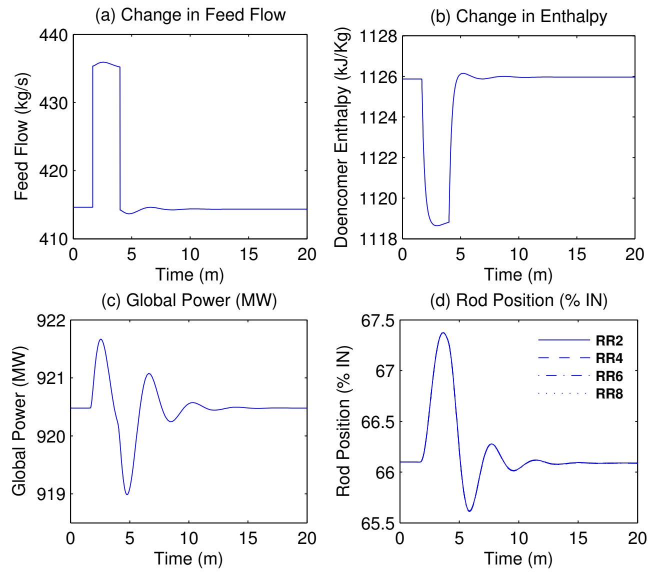

Fig. 7. Effect of temporary disturbance in the feed flow.

of 1.5 MW/s to 828.43 MW, in 61 s and held constant thereafter. During the transient, it is observed that, the global power is following the demand power as shown in Fig. 8. It is noted that, the xenon concentrations stabilizes to their respective new steady state values in about 40 h. However, the nodal powers attain the steady state value in about 100 s.

Further, the performance of controller is compared with three-time-scale approach presented by Shimjith et al. (2011a). In this case, RR6 was driven out manually by 2% giving appropriate control signal and simultaneously RR4 was driven in by 2%. Immediately after that regulating rods were driven back to their original positions. Result is generated for variations in control rod positions using both the controllers as shown in Fig 9. It is observed that, in both the cases RRs are driven back to their

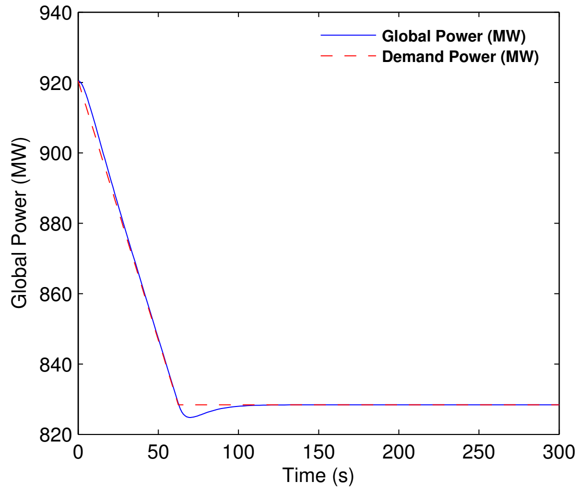

Fig. 8. Variation of global power during power maneuvering from 920.48 MW to 828.43 MW.

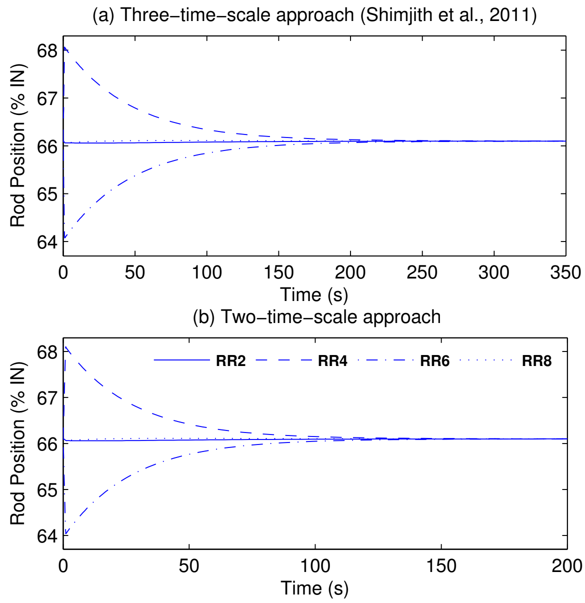

Fig. 9. Comparison of three-time-scale and two-time-scale methods.

equilibrium positions but time required to do so is less in the suggested controller. Variation in quadrant powers during this transient are given in Fig. 10.

5. CONCLUSION

In this paper, the original numerically ill-condition system of AHWR is decomposed into two lower order subsystems by singular perturbation technique. Linear quadratic regulators are then designed for the two subsystems separately and a composite controller for original system is obtained. This composite controller achieves an asymptotic approximation to the closed loop system performance and eliminates the ill-conditioning issues associated with AHWR. This controller is investigated for vectorized nonlinear model of AHWR. Performance of the suggested controller is judged via simulations carried out under various transient conditions. Proposed controller is compared with

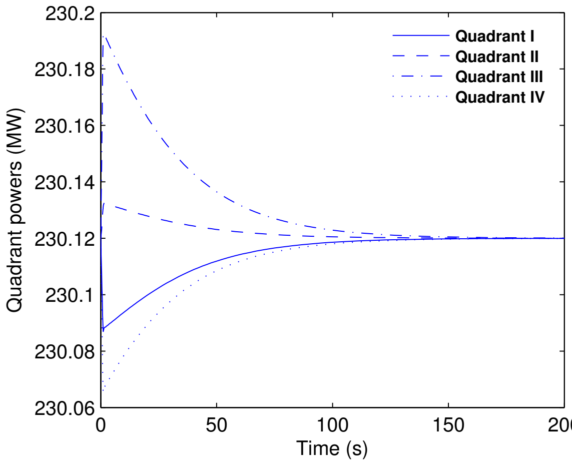

Fig. 10. Quadrant power variations during the transient.

three-time-scale composite controller for same transient levels. It is observed that performance of the suggested controller is better compared to three-time-scale composite controller in terms of spatial stabilization.

The control strategy for AHWR, presented here, utilizes the feedback of nodal powers, regulating rods' positions and xenon and iodine concentrations. For the later two variables, it would be necessary to employ an observer or estimator.

REFERENCES

Abbasi, A. R. and Wallam, F. (2014). Evaluating Transient Handling Capabilities of Fuzzy Logic Controller for a Pressurized Heavy Water Reactor. *Control Engineering and Applied Informatics*, Vol. 16, No. 2, pp. 40-48.

Astrom, K. J. and Bell, R. D. (2000). Drum-Boiler Dynamics. *Automatica*, Vol. 36, pp. 363-378.

Bobasu, E. and Selisteanu, D. (2003). Reduced Order Models for ElectroHydraulical Systems Control. *Control Engineering and Applied Informatics*, Vol. 5, No. 3,4, pp. 73-82.

Chow, J. H. and Kokotovic, P. V. (1984). A Decomposition of Near-optimum Regulators for Systems with Slow and Fast Modes. *IEEE Transactions on Automatic Control*, Vol. 21, pp. 701-705.

Duderstadt, J. J. and Hamilton, L. J. (1975). *Nuclear Reactor Analysis.* John Wiley & Sons Inc., New York.

Kokotovic, P. V., O'Malley, R. E. and Sannuti P. (1976). Singular Perturbation and Order Reduction in Control Theory-an Overview. *Automatica*, Vol. 12, pp. 123-132.

Londhe, P. S., Patre, B. M. and Tiwari, A. P. (2014). Design of Single-Input Fuzzy Logic Controller for Spatial Control of Advanced Heavy Water Reactor. *IEEE Transactions on Nuclear Science*, Vol. 61, pp. 901-911.

Munje, R. K., Londhe, P. S., Parkhe, J. G., Patre, B. M. and Tiwari, A. P. (2013). Spatial Control of Advanced Heavy Water Reactor by Fast Output Sampling Technique. *Proc. of IEEE International Conference on Control Applications, Hyderabad, India*, pp. 1212-1217.

Munje, R. K., Patre, B. M., Shimjith, S. R. and Tiwari, A. P. (2013). Sliding Mode Control for Spatial Stabilization of Advanced Heavy Water Reactor. *IEEE Transactions on Nuclear Science*, Vol. 60, pp. 3040-3050.

Munje, R. K., Patre, B. M. and Tiwari, A. P. (2014). Nonlinear Simulation and Control of Xenon Induced Oscillations in Advanced Heavy Water Reactor. *Annals of Nuclear Energy*, Vol. 64, pp. 191-200.

Munje, R. K., Patre, B. M. and Tiwari, A. P. (2014). Periodic Output Feedback for Spatial Control of AHWR: A Three-Time-Scale Approach. *IEEE Transactions on Nuclear Science*, Vol. 61, pp. 1-10.

Naidu, D. S. (1988). *Singular Perturbation Methodology in Control Systems.* Peter Peregrinus Ltd., London.

Phillips, R. G. (1980). A Two-Stage Design of Linear Feedback Controls. *IEEE Transactions on Automatic Control*, Vol. 25, pp. 1220-1223.

Saksena, V. R., O'Reilly J., Kokotovic, P. V. (1984). 'Singular Perturbation and Time-Scale Methods in Control Theory: Survey 1976-1983. *Automatica*, Vol. 20, pp. 273-293.

Shimjith, S. R., Tiwari, A. P. and Bandyopadhyay, B. (2008). Coupled Neutronics-Thermal Hydraulics Model of Advanced Heavy Water Reactor for Control System Studies. *Proc. of IEEE INDICON, IIT Kanpur, India*, 126-131.

Shimjith, S. R., Tiwari, A. P., Naskar, M. and Bandyopadhyay, B. (2010). Space-time Kinetics Modeling of Advanced Heavy Water Reactor for Control Studies. *Annals of Nuclear Energy*, Vol. 37, 310-324.

Shimjith, S. R., Tiwari, A. P. and Bandyopadhyay, B. (2011). A Three-Time-Scale Approach for Design of Linear State Regulator for Spatial Control of Advanced Heavy Water Reactor. *IEEE Transactions on Nuclear Science*, Vol. 58, pp. 1264-1276.

Shimjith, S. R., Tiwari, A. P. and Bandyopadhyay, B. (2011). Design of Fast Output Sampling Controller for Three-Time-Scale Systems: Application to Spatial Control of Advanced Heavy Water Reactor. *IEEE Transactions on Nuclear Science*, Vol. 48, pp. 3305-3316.

Shimjith, S. R., Tiwari, A. P., Bandyopadhyay, B. and Patil, R. K. (2011). Spatial Stabilization of Advanced Heavy Water Reactor. *Annals of Nuclear Energy*, Vol. 38, pp. 1545-1558.

Sinha, R. K. and Kakodkar, A. (2006). Design and Development of the AHWR-the Indian Thorium Fuelled Innovative Nuclear Reactor. *Nuclear Engineering and Design*, Vol. 236, pp. 683-700.

Syrmos, V. L., Abdallah, C. T., Dorato, P. and Grigoriadis, K. (1997). Static Output Feedback-A Survey. *Automatica*, Vol. 33, pp. 125-137.

Tiwari, A. P., Bandyopadhyay, B. and Govindarajan, G. (1996). Spatial Control of a Large Pressurized Heavy Water Reactor. *IEEE Transactions on Nuclear Science*, Vol. 43, pp. 389-402.

Tiwari, A. P. and Bandyopadhyay, B. (1998). Control of Xenon Induced Spatial Oscillations in a Large PHWR. *Proc. of IEEE International Conference on Global Connectivity in Energy, Computation, Communication and Control, New Delhi, India*, pp. 178-181.